Nanotechnology and Nano-Interface Controlled Electronic Devices
Editors: M. Iwamoto, K. Kaneto and S. Mashiko

CHAPTER 6

Polymer optoelectronics – towards nanometer dimensions

Olle Inganäs and Fengling Zhang

Biomolecular and organic electronics, Department of Physics and Measurement Technology, Linköping University, SE - 581 83 Linköping, Sweden

1. Introduction

The unification of the natural sciences in a form now widely being called nanosciences is one of the themes of the late 20th century scientific enterprise, and may well become a dominant theme in the 21th century. This reunification of the natural sciences, divided by processes of specialisation in the late 19th century, is central to the development of the field of conjugated polymers at the junction of physics and chemistry. Here chemistry delivers materials in the forms of conjugated polymers and molecules, using well-established methods of synthetic organic chemistry and polymer chemistry. The objects of synthesis are defined on the Å and nm length scale, and are synthesised in samples carrying millimoles of objects. The objects are quasizero- or one-dimensional electronic systems with a high degree of excitation and charge confinement, but also with a high mobility on the nm length scale. Physics offer one description of the electronic structure of these systems, complementary to the quantum chemical description but all based in quantum mechanics; the language in which these objects are described may however differ between chemistry and physics. The description of the excited states, so crucial to the development of optoelectronic devices for emission of light by

electronic injection of charge into molecules and polymers, or for creation of charges from excited states, is an area of controversy, and where physical and chemical models meet and collide. While these models may be fought over, using sophisticated models and spectroscopies, there is in the background a steady development of new molecules, materials and devices, which sometimes leads to results contradicting current dogma. A particular enigmatic example of these controversies is the issue of charge recombination in organic layers, where a simple argument from symmetry shows that electrons and holes recombining in a solid should lead to singlet and triplet excited states in a ratio of 1 : 3. More recent experimental determinations do not agree with this rule [1], and the ratio has been shown even to go beyond 1 : 1. As the ratio is now considered to be a material and device parameter, rather than a fundamental property of recombining charges, one of the ultimate limiting factors of light emitting diodes is no longer present. Likewise, in the field of organic photodiodes, a central issue is the binding energy of the excited state, as it has a clear impact on the formation of mobile charges in photodiodes. No clear consensus is yet found, and the range of binding energies reported from experimental studies is broad. Internal quantum efficiencies of excited state dissociation into charges can be very high in donor–acceptor systems, and the kinetics of these processes is extremely fast [2]. In pure homopolymer systems, routes towards photogeneration of charges are present [3], but much less efficient than what is found in donor–acceptor complexes where an electron acceptor receives an electron from the excited state on a conjugated polymer or molecule [4,5]. However, progress in organic photodiodes has now generated photodiodes with external quantum efficiency at low intensity monochromatic illumination of better than 60%, and solar cells with solar energy efficiencies of 2.5% at AM 1.5 conditions [6–9]. A steady development of new materials, new devices and new patterning methods contributes towards incremental progress in this field. The length appropriate for analysis and characterisation in this field spans from the Å and nm level, for chemical structure in donor–acceptor moieties, to 1–10 nm for the diffusion of excited states and charge carriers, to 10–100 nm for the description of multilayer devices where a photoactive solid is confined between electrodes separated by this thickness, and to 100–1000 nm, where electrodes and photoactive solids are patterned on this length scale for trapping and confining light. Looming in the background are found also the large area devices, which are deposited as thin films on flexible carriers of cm to dm dimensions, and which may one day be found as an organic solar cell for energy conversion. Here conditions for large or giant area electronics are crucial, and it is of great importance to develop green chemistry and large area deposition methods. This chapter focuses on some of our recent contributions to the field of organic photodiodes, with particular emphasis on the nanometer dimensions of materials, processes and devices.

2. Excited states in polythiophenes

We have chosen polythiophenes (PT) as our main group of conjugated polymers for photovoltaics [10]. The molecular structures of polythiophenes (PT) are shown in Fig. 1. This choice is because this family of polymers is very versatile from the point of view

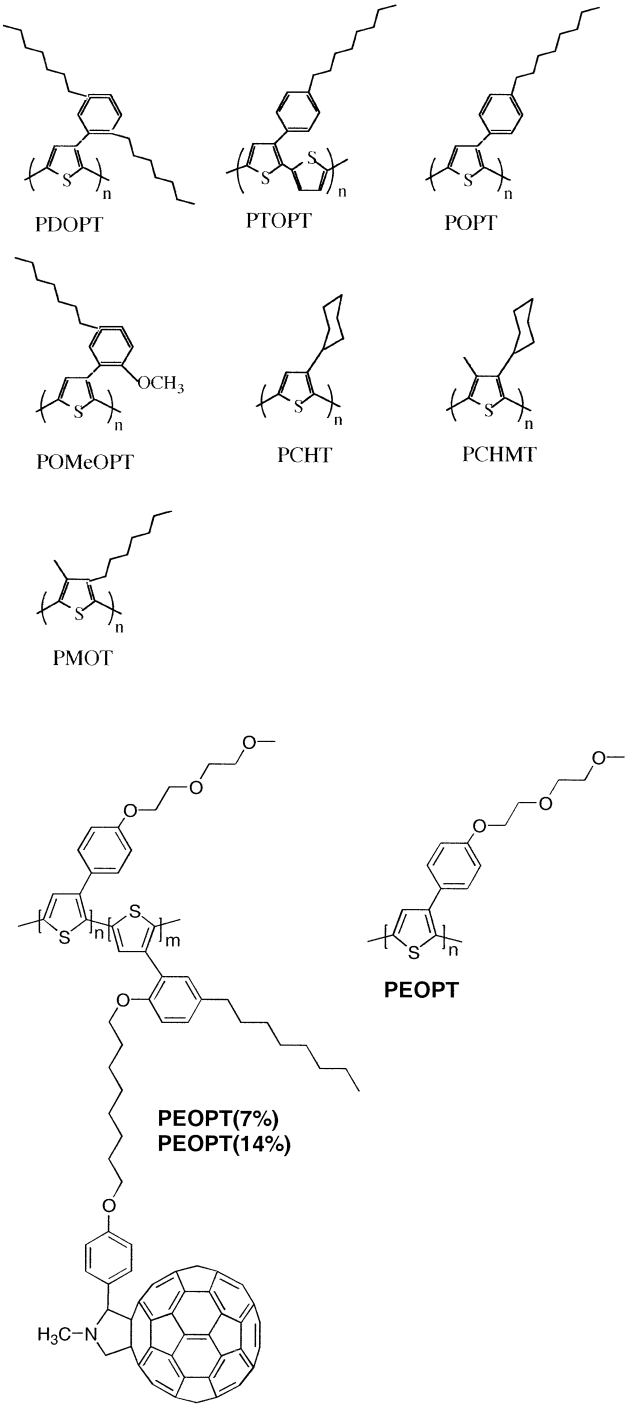

Fig. 1: The chemical structures of polythiophenes and a copolymer, some of which are used in photodiodes. The copolymer [22] demonstrates covalent linking of polymer donor and acceptor.

of polymer modification by chemical substitution, and from the point of view of the higher photostability of polythiophenes as compared to poly(paraphenylene vinylenes), for example. It is thus quite easy to move the optical absorption over much of the visible spectrum, and the range of polythiophenes covers a sizable part of the solar spectrum. Another reason is the possibility of making high mobility polymers, as shown in recent years where poly(alkylthiophenes) have been induced to have high field effect mobility in polymer transistors, and even the possibility to field dope into the metallic and superconducting regime [11].

The nature of the excited state in PTs has been extensively studied through photoluminescence (PL) quantum yield and photoluminescence and photoinduced absorption kinetics [12,13]. The radiative lifetime of the excited state is typically 1–2 ns, and one source of decay is through internal conversion. That process is much enhanced in poly(alkylphenylthiophenes) designed for a non-planar geometry and high bandgap [12]. As these polymers do not give much absorption in the solar spectrum, they are less significant for photovoltaics. More important are the low bandgap PTs, where aggregates have been shown to lead to non-radiative recombination of excited states [13]. These non-radiative processes are not sufficiently fast to outcompete the process of photoinduced charge transfer in photodiodes. The possibility of intersystem crossing in PTs, induced by the spin–orbit coupling due to the presence of a sulphur atom in the carbon conjugated chain, is of little importance in photovoltaics, as it appears that both singlets and triplets may be dissociated by the presence of acceptors.

The diffusion of the excited state is much influenced by the chemical structure of the polymer, as well as by the morphology of the polymer when aggregating into solid films. The typical behaviour is a drastic loss of PL quantum yield upon precipitation of PTs from good solvents. There are important alternatives; we have observed an enhanced PL yield of some soluble polythiophenes [14] when decreasing the solvent quality on the route to the solid, where once more a general reduction of PL yield is found. It may be that special aggregation forms may retain and even increase the quantum yield, but most forms of aggregation lead to an increase of the non-radiative decay and thus quench luminescence. The spectral migration of excited states reveals a diffusion of these, which will couple the excited state to some source of non-radiative recombination, which is never far away in a polymer film. Copolymers and oligomers incorporating chemically modified thiophene units have been shown to have a much enhanced PL quantum yield [15].

The geometry of the polymer chain in good solvents has been studied by photophysical methods, where a sub-picosecond pulse of (polarized) monochromatic light is used to excite polymer chains in solid films or in solutions; during the coming picoseconds the intensity or polarisation state of the rapidly decaying luminescence is observed. In these studies is revealed how transport of the excited state along the single polymer chain in a dilute solution in a good solvent occurs [16]. This study reveals a tendency of the low bandgap PTs to give a stiff, close to planar, geometry as expected from the point of theory. When now packing these chains into a polymer solid, a memory of the chain conformation in the solvent may persist, as argued in other studies.

3. Diffusion length of excited states

In the solid state, the length of diffusion of the excited state is one of the important parameters controlling the design of photodiode materials. If the excited state is capable of finding a site for non-radiative recombination prior to finding a site for photoinduced charge transfer, potential photocurrent is lost. Determination of the exciton diffusion length is therefore an important item.

We have used a combination of photoluminescence measurements and optical modelling to deduce the diffusion length of the excited state which can be quenched by the presence of C60 molecules [17]. In order to be able to do this experiment, we have chosen a polythiophene, which does not easily dissolve fullerene compounds, as to be able to obtain sharp bilayers of polythiophene/C60, where the fullerene is evaporated onto a thin spin-coated polymer film, carried on a quartz substrate. These methods of deposition give reasonably flat films, and these films can be used to obtain the full dielectric function of the materials. To do this we use spectroscopic ellipsometry, a non-invasive method of high precision, which will also measure the thickness of films. We also determine the absolute PL quantum yield of these bilayers, in integrating sphere measurements, and vary the polymer and C60 thickness. As the thickness of the polymer films increases, more excited states are created at a distance from the polymer/C60 junction, and higher PL is obtained. With these methods, and with a detailed optical model of the thin film optical physics valid in films of 10–100 nm thickness (Fig. 2), we are able to determine the diffusion length of the excited state. We find that to be 5 nm in the polymer studied. This is the distance in which an acceptor must be found in order for an excited state to be able to generate charge. The diffusion length is a materials property, and may also be influenced by morphology and packing of chains. It is therefore an object of design and synthesis.

Fig. 2 shows the distribution of absorbed electromagnetic energy from an incident monochromatic wave at a polymer/C60 bilayer supported on a semi-infinite quartz layer. The internal reflection of waves inside the bilayer gives a different excitation distribution compared to that obtained from a simple-minded application of the Lambert–Beer law as often used. The excitation or exciton distribution is actually not completely identical to the distribution of excited states formed by absorption, as exciton diffusion may have an impact, in particular close to boundaries. Even more is this physics relevant in the emission of photons from excited states within the polymer layer, a distribution that must also be included in the complete analysis of the emission profile versus wavelength in the far field.

We may also approach this problem of quenching of excited states in the presence of acceptors by constructing objects where the excited state should always find an acceptor within that distance. A realisation of such elements is found in the double-cable polymers, so named because a polymer is carrying both an electron acceptor and an electron donator [18–22]. These elements are also necessary for the further transport of photogenerated charges, as they will hop between occupied and unoccupied states on the electron acceptor moiety and electron donor moiety, respectively. The term double cable refers to this property, and by incorporation of these elements on each polymer chain means for excited state dissociation and for charge transport are found everywhere in the material.

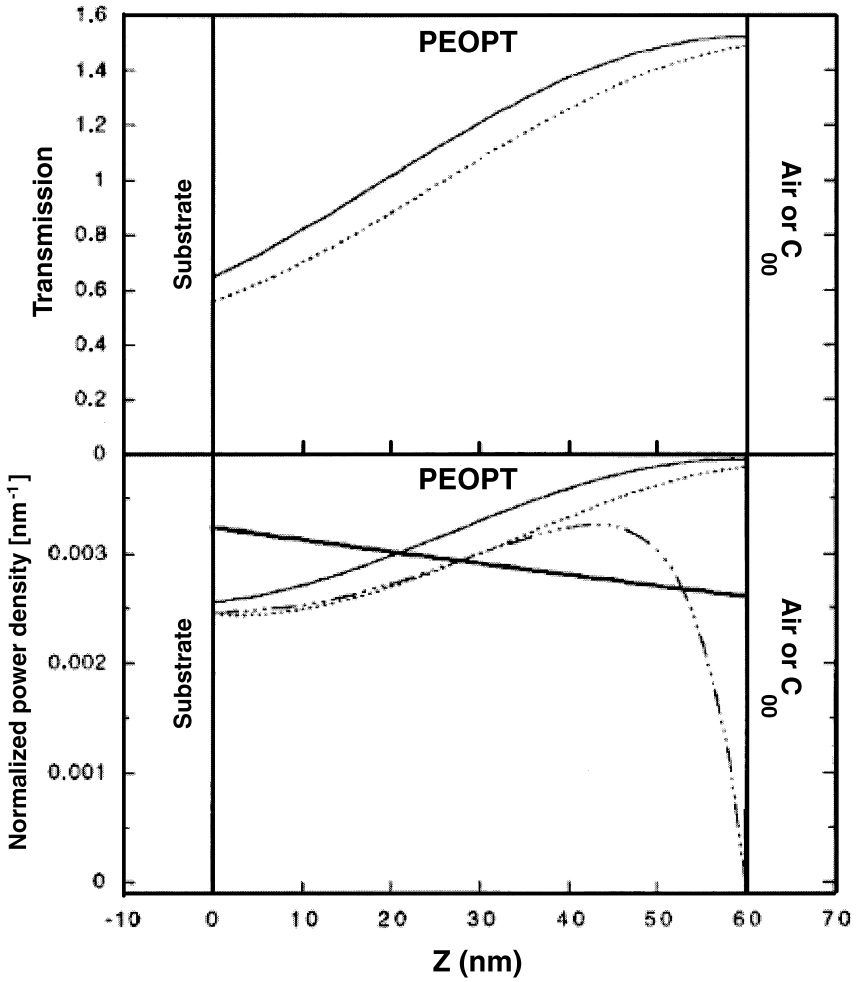

Fig. 2: The lower panel shows the calculated power excitation density $g(z)$, of a 60 nm polymer film excited at 2.34 eV, normalised to the incoming intensity. The axes thus show the fraction of the incoming intensity absorbed per length unit. The different lines are the absorbed power density for a neat film (thin solid line) and a polymer film with a 4 nm film of C60 on top (dashed line). The excitation density assuming an exponential decay of the incoming radiation (e.g. $I = I_0 \mathrm{e}^{-\alpha z}$) is shown (thick solid line). Also shown is the steady-state power density with an infinite sink at the polymer/C60 heterojunction and a diffusion length of 5.3 nm (broken dashed line). The upper panel shows the calculated transmission of the polymer emission from different points z in the polymer film, to a point outside the quartz substrate (see text for more details). The transmission is shown for the case of a neat polymer film (thin solid line) and a polymer film with 4 nm C60 on top (dashed line). (From Ref. [17].)

A recent example of double cable polymers is found in a soluble polythiophene–C60 copolymer, where copolymerisation of substituted thiophenes with a fraction of C60 carrying substituted thiophenes leads to the polymer. Photoinduced charge transfer is easily observed in these polymers, and is almost complete in the solid and partial in the

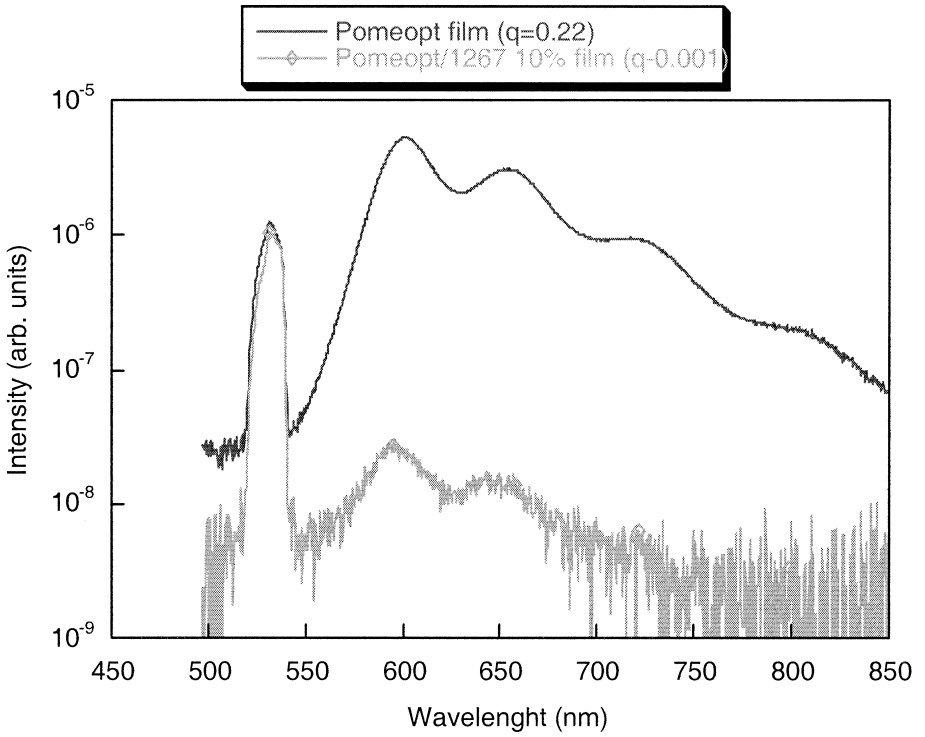

C60(%)	PL(%)
0	22
10	≈0,1

Fig. 3: PL spectra and their PL yield from pure POMeOPT film and copolymer POMeOPT with 10% C60 film show the PL quenching in copolymer film of POMeOPT.

solution of the polymer. Fig. 3 shows the PL quenching in one of these copolymers. Variation of the stoichiometry of the polymer can be used to enhance the quenching; unfortunately the solubility of the polymer is not retained when putting more than one C60 per 4 monomers of thiophene in the copolymer. The processing through polymer solutions is crucial to obtain thin film devices, which are required for good devices. We are, however, free to enhance the C60 concentration in these polymers by mixing

C60 into a common solvent. This will lead to polymer films with enhanced photodiode performance [22], indicating that the density of C60 is not sufficient in the copolymer per se.

4. Stratified photodiodes

The sequel to photoinduced charge separation in photodiodes is the transport of generated charges to the electrodes. This should preferably happen without the trapping or recombination of these charges, which are very plausible events in the materials concerned. Localisation of charges into traps is very likely due to the high degree of disorder; recombination is likely when a stream of charges passes through fixed space charges of the opposite polarity. It is therefore essential to organise the paths of the electron and hole so that they can be transported with minimal trapping and recombination.

Blends of donor and acceptor do not always deliver this. The size of domains in which donors and acceptors are aggregated is influenced both by kinetics and statics of blending, and it is expected and observed that the mode of preparation of these blends, and layers from blends in solutions, should have a major impact on the performance of devices. The process of removing solvent from a blend may be fast – as in spin-coating – or slow, such as in dropcasting or doctor blading. The phase structure of the resulting film is probably very different under these different circumstances. We note that the highest solar cell efficiencies are reported [9] for films prepared from particular blends of solvents, where the change of composition during evaporation of the different solvents at different rates is yet another mechanism that will influence the kinetics of thin film formation and molecular organisation/morphology in the film. By influencing the degree of phase separation by purely chemical means, as for example when using a "immobilised solvent" as a side chain of a polythiophene, molecular miscibility of polymer/C60 is obtained, and the resulting phase structure does not show up above 20–30 nm [23].

To gain some small means of control of the 10–100 nm organisation of materials in the vertical dimension, we have developed stratified photodiodes [24,25]. These are assembled by using a soluble fullerene derivative to be spin-coated on top of a polymer film, previously deposited by spin-coating on a substrate. The structure of the stratified active layer in photodiodes is shown in Fig. 4.

The second act of spin-coating could of course be expected to dissolve the first layer, unless solvents and conditions are carefully chosen so as not to dissolve the first layer when depositing the second. This has been possible for bilayers of high molecular weight PPV and soluble methanofullerene compounds, which form graded junctions [25]. The diffuse junctions of the polymer phase at the bottom, with a methanofullerene phase on top, is much more effective in generating photocurrent. This is very visible in the photoluminescence of the polymer layer, which is almost completely quenched in the presence of the methanofullerene, this indicating a very effective dissociation of excited states. The increase of photocurrent, due to the higher contact area between donor and acceptor molecules, now must be transferred through layers, which eventually

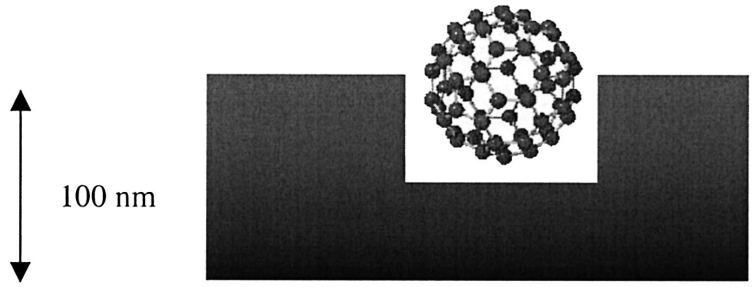

Fig. 4: A cross section of the stratified active layer of polymer and C60 in stratified photodiodes.

end up in polymer only contacts at the anode side, and methanofullerene only contacts at the cathode side.

5. Excitation transfer in photodiodes

The collection of optical energy is in green plants very much helped by the construction of the photosynthetic apparatus. Here antenna pigments in a primary step absorb the incoming photons. That energy is transferred to a reaction center chlorophyll in reaction centers PSI and PSII, wherein the primary photochemistry occurs. The nature of these antenna pigments varies, and they may be chlorophylls but they may also be distinctly different, for instance in the form of xanthenes. The collection of energy from antenna pigments to reaction center chlorophyll occurs through excitation transfer, also known as Förster transfer. One advantage of this system is that more of the photon flow may be absorbed, through the use of pigments of different absorption spectra. The same advantage is something we would like to utilise in photodiodes, to sensitize some part of the green and blue part of the solar spectrum. This requires the use of several pigments, and we have implemented this in the form of polymer blends. In a study of three different red polythiophenes – absorbing in the green part of the spectrum – in combination with a polyparaphenylene vinylene absorbing in the blue-green, we have demonstrated that this principle may be used to enhance the action spectrum of the photodiodes [26].

These devices were built as bilayer photodiodes, where an evaporated C60 layer is the acceptor located on top of a polymer blend layer. We compare the performance of photodiodes incorporating blends with photodiodes where the polymer layer is a homopolymer. The high bandgap polymer shows an emission spectrum largely overlapping with the absorption spectra of the lower bandgap polythiophenes. By studying the photoluminescence spectrum of homopolymers and blend, we establish that almost complete excitation transfer occurs in the polymer blends of 1 : 1 (by weight). This is very visible in the complete suppression of emission from the PPV high bandgap polymer, and in the considerable enhancement of PL from the polythiophenes used. This enhancement is very visible as the emission intensity from the three different polythiophenes is not high. Photoluminescence and excitation transfer in photodiodes is

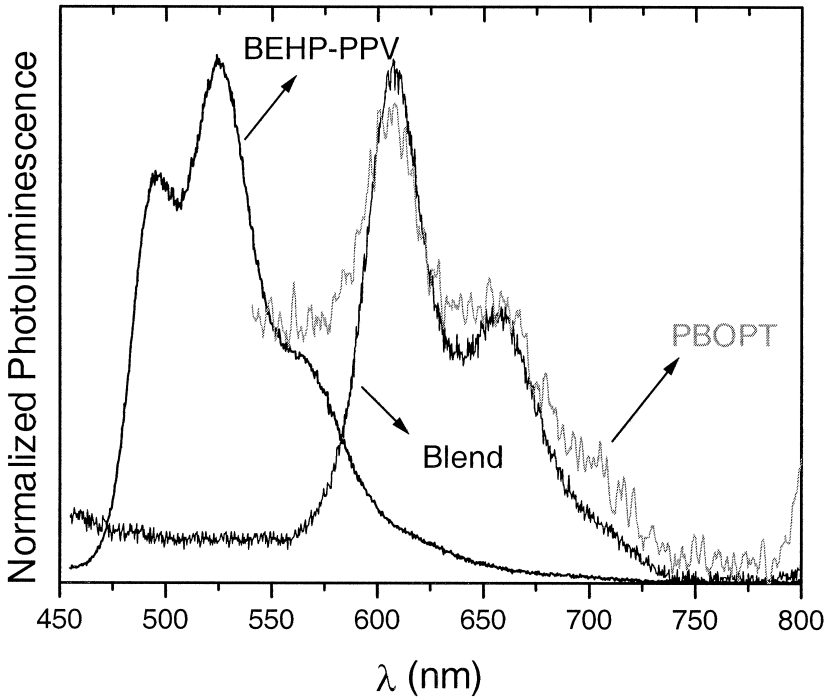

Fig. 5: PL spectra of polymeric films of BEHP-PPV, PBOPT and the blend BEHP-PPV : PBOPT in the ratio 1 : 1.

shown in Fig. 5. Therefore we conclude that geometries suitable for excitation transfer are obtained in these blends obtained by spin-coating from a common solvent. We corroborate this interpretation by imaging the blend layer surface in scanning force microscopy, with the tapping mode of interaction between tip and surface. We are unable to resolve any fine-structure in these blends, which may be due to structures being smaller than the limits of resolution of the method, say 20–30 nm, or by a complete phase separation into a pancake geometry, where one of the polymers would be residing on top of the other. This does not appear to be a likely geometry, but is not excluded by our studies. The total absorption of the film is such as to make implausible that the degree of excitation transfer that is observed could be originating from a double layer, as the individual layers would have to be too thin to generate the optical absorption observed. It is therefore plausible that the dimensions of phase separation are small, and that most PPV chains are found close enough to a PT chain to allow excitation transfer.

In photodiodes incorporating polymer blends we find consistently higher photocurrents and lower photovoltages. The photovoltages observed are similar to those that would be found in homopolythiophene/C60 layers, and we therefore conclude that photocurrent generation occurs through excitations found on the polythiophene chains, but to some degree delivered there by excitation transfer from the PPV. An enhancement

of photocurrent and an extension of the action spectrum is the result. We may in this case argue that the characteristic length of Förster transfer is smaller or comparable to the phase separation dimensions. Later and more extensive studies of polymer blends in other polymer families have revealed a multitude of length scales in the phase separation between two polymers [27,28].

6. Models of charge generation in photodiodes

The same thin film optical phenomena found valuable in the analysis of photoluminescence quenching in polymer/C60 bilayers is also of importance in analysing the performance of photodiodes constructed by sandwiching this bilayer in between two electrode layers, one metallic and highly reflective and one conducting but almost transparent [29,30]. For all the materials in this photodiode, dielectric functions have been measured with the help of spectroscopic ellipsometry. With help of a detailed optical model of all internal reflections and transmission at internal boundaries, we are able to calculate the distribution of optical energy of the incoming (and partly reflected) wave. Fig. 6 shows the distribution of optical energy in photodiodes with different thicknesses of C60. The distribution of optical absorption is thus known, and we can couple this to the generation of photocurrent in the device by including this distribution as a source term in a diffusion equation appropriate for neutral excited states. With fixed thickness and optical parameters, due to the spectroscopic ellipsometrical data, we have only one free variable in fitting our real data of the external quantum efficiency of the devices; that is the diffusion length of the excited state contribution to the formation of photocurrent. We implicitly assume many things, in particular that the photoinduced charge transfer occurs only at the interface between polymer and C60. This assumption is identical in PL quenching modelling experiments, and both types of experiment end up with an exciton diffusion length of 5 nm. Considering this short distance, we note that we must position all polymer chains within a distance of less than 5 nm in order to transfer the excitation energy. This may not be a common situation in polymer blends.

7. Nanodimension of electrodes

In developing nanoelectronic devices based on polymers, the electrodes must be patterned at a sub-micron scale; the vertical dimension of the device is almost always less than a few hundreds of nm. In order to pattern at a nano scale, in addition to the traditional photolithography processing, soft lithography was developed and is nowadays used as a suitable method for patterning polymers [31,32]. Micro- or nano-patterning of polymers is not only necessary for electrical addressing and wiring of the circuits, but also has other functions, such as trapping more light to improve the performance of polymer photodiodes [33] or increasing the efficiency, and controlling light output from microstructured LEDs [34,35].

The conducting polymer poly(3,4-ethylenedioxythiophene) doped with poly(4-styrenesulfonate) (PEDOT-PSS) is often used as a metal in polymer electronic devices,

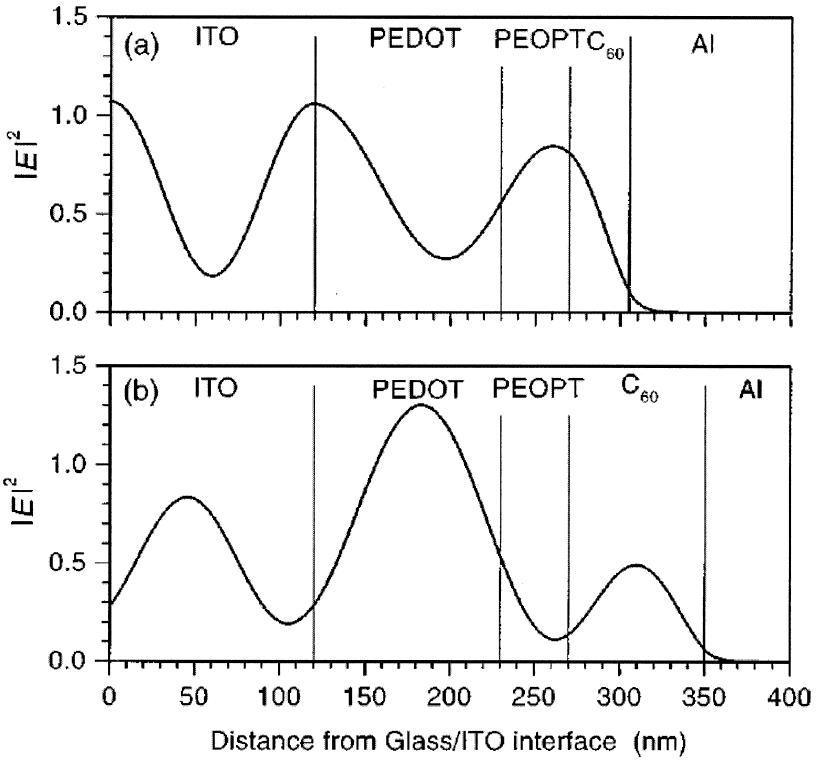

Fig. 6: Calculated distribution of the normalised modulus of the optical electric field $|E|^2$ inside a photovoltaic device: glass (1 mm)/ITO (120 nm)/PEDOT (11O nm)/PEOPT (40 nm)/C60/Al with a C60 layer thickness of (a) 35 nm and (b) 80 nm for a wavelength of 460 nm.

as a modified anode on top of indium tin oxide (ITO), in photodiodes of enhanced performance [36] and for improvement of the rectification ratio in polymer diodes PEDOT-PSS can be modified with glycerol or sorbitol to increase the conductivity by two orders of magnitude. This makes it possible to use this material as a flexible electrode for application in optoelectronic devices. The PEDOT-PSS has double functions in electronic devices: to enhance the electrode performance by adjusting the work function of an electrode [37] and for use as a flexible anode [38]. We here introduce our experimental results on nano-patterning of conducting polymer PEDOT-PSS, both on glass and Si wafer, patterned by a soft lithography technique, MIMIC and liquid printing, which we believe are new approaches for obtaining polymer nanostructures. These could have potential application in biology and optoelectronics.

Nanowires of PEDOT-PSS was fabricated from its aqueous solution on glass or Si wafers, by using capillary action in MIMIC structures. Two different elastomer submicron patterns were made by casting polydimethylsiloxane (PDMS) onto commercially available diffraction gratings. We put the elastomer stamp in conformal contact with a piece of cleaned glass or an Si wafer, and then applied a drop of PEDOT-PSS (Baytron P, Bayer AG, concentration 1.3%) aqueous solution in front of the capillary openings of

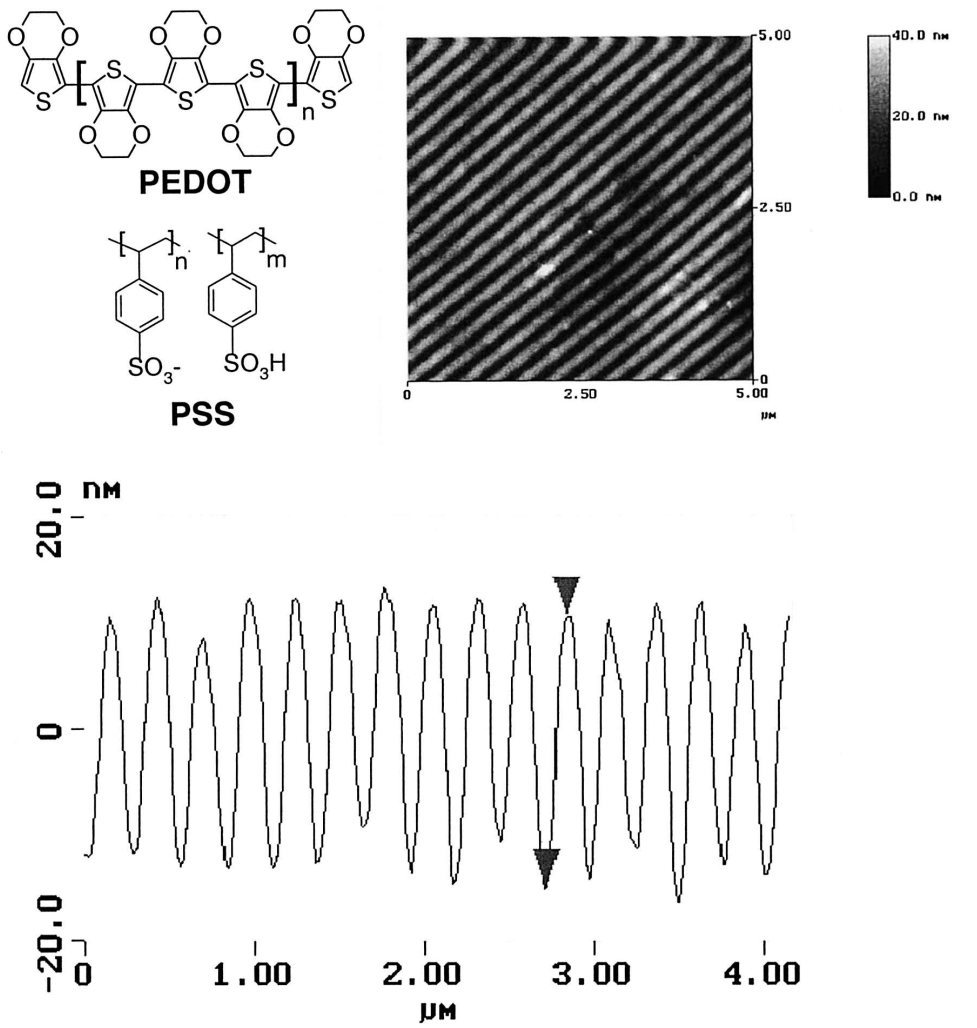

Fig 7: SFM image of polymer PEDOT-PSS nanowires and chemical structure of PEDOT-PSS. The period of the nanowires was 270 nm and the height ≈25 nm. The cross section picture shows the profiles of the wires and their height.

the stamp. The sample was then left for several hours, for the solution to migrate into the capillaries and subsequently dry out. After the solution had dried we carefully peeled off the stamp leaving the polymer nanowires standing on the surface. In this way the grating pattern was transferred from the stamp to the polymer layer. All the processes were performed in ambient condition.

A scanning force microscope (SFM-Nanoscope III, Digital Instruments) was used in tapping mode to image the polymer nanowires. Fig. 7 shows SFM images of polymer PEDOT-PSS nanowires (3600 lines per millimeter) with the same period as the stamp

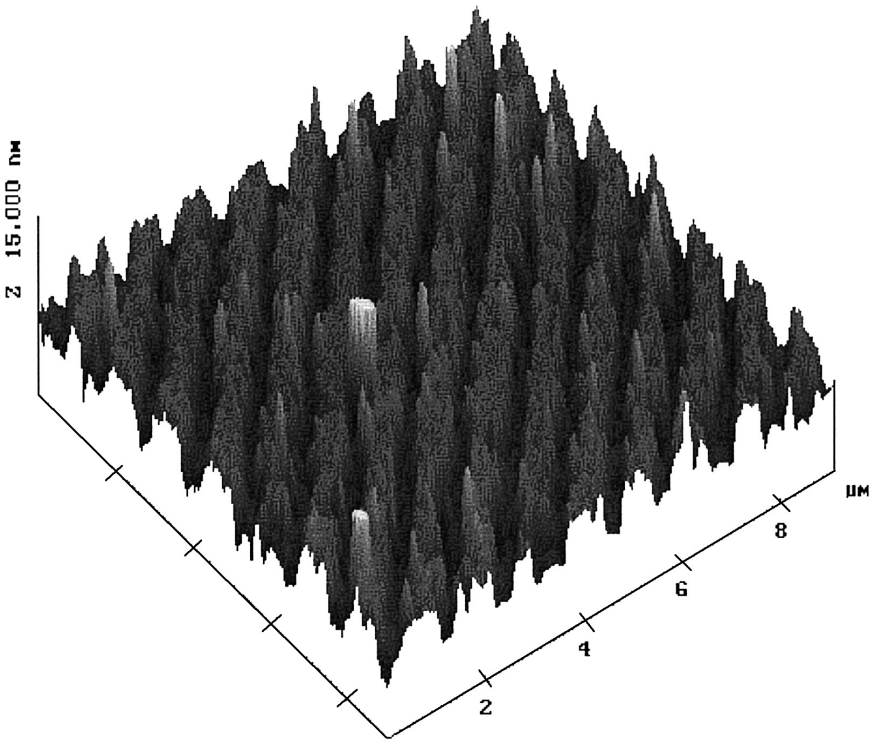

Fig. 8: SFM image of nanowires with a period 833 nm molded with a compressed stamp, showing a height of the nanowires of ∼8 nm and a width of ∼600 nm with a separation of 200 nm.

(280 nm), but with a lower height (∼25 nm) after drying than the depth of the original stamp (∼55 nm).

In order to make polymer nanowires of lesser height, we desired to reduce the size of the capillary channel. This we did by placing a weight (≈100 g), resulting in a pressure of ∼10 kPa on top of the stamp to compress the channel during molding. The pressure we used to deform the stamp is similar to that previously analysed [39]. We also diluted the PEDOT-PSS solution with distilled water (1 : 1). Si wafer was used instead of glass to decrease the roughness of the substrate. The SFM images show that the height of the lines resulting in the MIMIC process could be decreased, depending on the pressure exerted on the top of the stamp. For example, the height of the nanowires for the 1200 grating under zero load is 70 nm, which decreased to around 8 nm during loading with ∼10 kPa (see Fig. 8). The top of the wires was deformed under these conditions. The nanowires in Fig. 8 are separate from each other, the distance between lines is ∼200 nm and the width of the wires is around 650 nm. The lengths of the nanowires can reach 1 cm.

8. Nano-pattern application in photovoltaic devices

In polymer photovoltaic devices, the thickness of the diodes is crucial. To absorb more light a thick film is needed, but due to the low mobility of charge carriers, this is associated with increasing series resistance. In bilayer diodes built from the combination of an electron donor and acceptor, the excited state dissociates at the interface between electron donor layer and acceptor layer. The larger interface area thus causes more efficient charge separation. These two aspects of device thickness motivate efforts to combine donor and acceptor in micro and nano-patterned diodes, to control the geometry and thus influence photon propagation in the device as well as to control the interface area between donor and acceptor. We have used soft embossing to pattern active polymer layer to enhance the external quantum efficiency (EQE) of photodiodes [33]. Here we combine two soft lithography methods, liquid printing and soft embossing, to fabricate the devices with two periodic patterns to increase the performance. Metallic polymer anode PEDOT-PSS was micro patterned in 600 lines/mm and polythiophene POMeOPT layer was nano-patterned in 3600 lines/mm followed by vacuum deposition of C60 as electron acceptor to keep a sharp interface. The bilayer diodes were fabricated as ITO/PEDOT-PSS/POMeOPT/C60/Al. Our results show that the EQE of these diodes with patterned anode and polymer was enhanced compared with non-patterned planar diodes (see Fig. 9). These results demonstrate the possibility of using sub-micro and nano-pattern by soft lithography to implant structure in polymer photodiodes to improve light trapping in thin active layers, so that the performance of these devices may be enhanced.

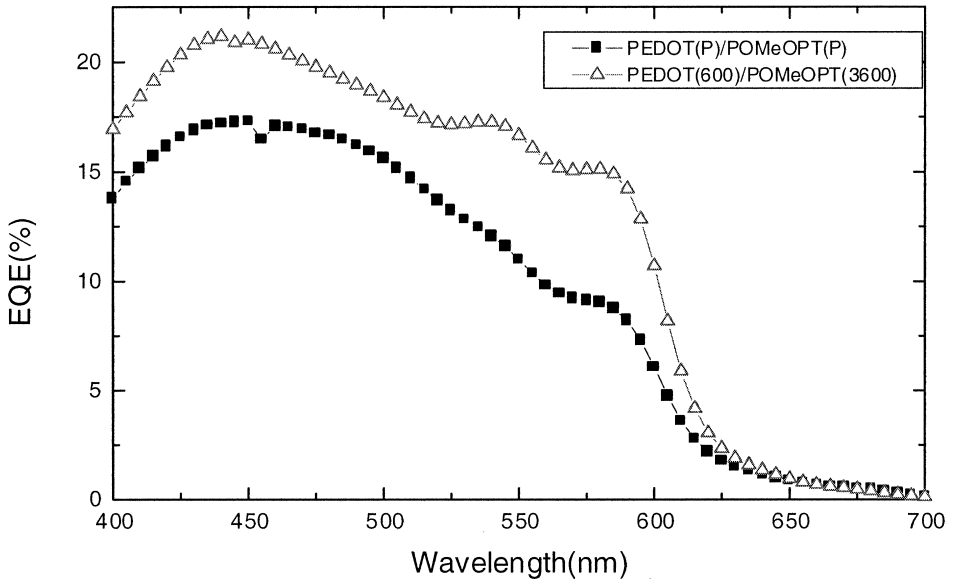

Fig. 9: The EQE of photodiodes with pattern PEDOT-PSS in 600 lines/mm, pattern polymer (POMeOPT) in 3600 lines/mm (open triangles) and planar PEDOT-PSS, planar POMeOPT (filled squares).

In summary, we have demonstrated how processes and structures with nanometer extension are crucial to the operation of polymer photodiodes. Structuring of materials on the nanometer length scale is thus an important tool for obtaining higher detection and conversion efficiencies in these devices, always relying on parallel progress in chemical synthesis, materials formulation and device assembly.

Acknowledgements

We wish to acknowledge all the coworkers and students contributing to the studies here reported, in particular Lucimara Stolz Roman, Lichun Chen, Mathias Theander, Leif Petterson, Yohannes Teketel and many more. Joint European projects with S. Sariciftci, C. Brabec, J. Hummelen, R. Janssen, M. Maggini, M.R. Andersson and M. Prato have been instrumental in delivering materials. Fundings from the Göran Gustafsson foundation and the Carl Tryggers foundation have been instrumental to achieve these results, as well as the Engineering Research Board (TFR).

References

1. Y. Cao, I.D. Parker, G. Yu, C. Zhang, and A.J. Heege, Nature **397**, 414 (1999).
2. C.J. Brabec, G. Zerza, G. Cerullo, S. De Silvestri, S. Luzzati, et al., Chem. Phys. Lett. **340**, 232 (2001).
3. A. Ruseckas, M. Theander, M.R. Andersson, M. Svensson, M. Prato, et al., Chem. Phys. Lett. **322**, 136 (2000).
4. N.S. Sariciftci, L. Smilowitz, A.J. Heeger, and F. Wudl, Science **258**, 1474 (1992).
5. G. Yu, J. Gao, J.C. Hummelen, F. Wudl, and A.J. Heeger, Science **270**, 1789 (1995).
6. C.J. Brabec, N.S. Sariciftci, and J.C. Hummelen, Adv. Func. Mater. **11**, 15 (2001).
7. C.J. Brabec and S.N. Sariciftci, Monatsh. Chem. **132**, 421 (2001).
8. O. Inganäs, L.S. Roman, F.L. Zhang, D.M. Johansson, M.R. Andersson, and J.C. Hummelen, Synth. Metals **121**, 1525 (2001).
9. S.E. Shaheen, C.J. Brabec, N.S. Sariciftci, F. Padinger, T. Fromherz, and J.C. Hummelen, Appl. Phys. Lett. **78**, 841 (2001).
10. M.R. Andersson, O. Thomas, W. Mammo, M. Svensson, M. Theander, and O. Inganäs, J. Mater. Chem. **9**, 1933 (1999).
11. J.H. Schon, A. Dodabalapur, Z. Bao, C. Kloc, O. Schenker, and B. Batlogg, Nature **410**, 189 (2001).
12. M. Theander, O. Inganäs, W. Mammo, T. Olinga, M. Svensson, and M.R. Andersson, J. Phys. Chem. B **103**, 7771 (1999).
13. A. Ruseckas, E.B. Namdas, T. Ganguly, M. Theander, M. Svensson, et al., J. Phys. Chem. B **105**, 7624 (2001).
14. M. Theander, M. Svensson, A. Ruseckas, D. Zigmantas, V. Sundstrom, et al., Chem. Phys. Lett. **337**, 277 (2001).
15. G. Gigli, O. Inganäs, M. Anni, M. De Vittorio, R. Cingolani, et al., Appl. Phys. Lett. **78**, 1493 (2001).
16. M.M.L. Grage, T. Pullerits, A. Ruseckas, M. Theander, O. Inganäs, and V. Sundstrom, Chem. Phys. Lett. **339**, 96 (2001).
17. M. Theander, A. Yartsev, D. Zigmantas, V. Sundstrom, W. Mammo, et al., Phys. Rev. B **61**, 12957 (2000).
18. A. Cravino, G. Zerza, M. Maggini, S. Bucella, M. Svensson, et al., Chem. Commun. **24**, 2487 (2000).
19. A. Cravino, G. Zerza, H. Neugebauer, S. Bucella, M. Maggini, et al., Synth. Met. **121**, 1555 (2001).

20. A. Cravino, G. Zerza, H. Neugebauer, M. Maggini, S. Bucella, et al., J. Phys. Chem. B **106**, 70 (2002).
21. G. Zerza, A. Cravino, H. Neugebauer, N.S. Sariciftci, R. Gomez, et al., J. Phys. Chem. A **105**, 4172 (2001).
22. F.L. Zhang, M. Svensson, M.R. Andersson, M. Maggini, S. Bucella, et al., Adv. Mater. **13**, 1871 (2001).
23. l.S. Roman, M.R. Andersson, T. Yohannes, and O. Inganäs, Adv. Mater. **9**, 1164 (1997).
24. D. Godovsky, L.C. Chen, L. Pettersson, O. Inganäs, M.R. Andersson, and J.C. Hummelen, Adv. Mater. Optics Electr. **10**, 47 (2000).
25. L.C. Chen, D. Godovsky, O. Inganäs, J.C. Hummelen, R.A.J. Janssens, et al., Adv. Mater. **12**, 1367 (2000).
26. L.C. Chen, L.S. Roman, D.M. Johansson, M. Svensson, M.R. Andersson, et al., Adv. Mater. **12**, 1110 (2000).
27. A.C. Arias, J.D. MacKenzie, R. Stevenson, J.J.M. Halls, M. Inbasekaran, et al., Macromolecules **34**, 6005 (2001).
28. A.C. Arias, N. Corcoran, M. Banach, R.H Friend, J.D. MacKenzie, and W.T.S. Huck, Appl. Phys. Lett. **80**, 1695 (2002).
29. L.A.A. Pettersson, L.S. Roman, and O. Inganäs, J. App. Phys. **86**, 487 (1999).
30. L.A.A. Pettersson, L.S. Roman, and O. Inganäs, Synth. Met. **102**, 1107 (1999).
31. Y.N. Xia and G.M. Whitesides, Angew. Chem. Int. Ed. **37**, 551 (1998).
32. E. Kim, Y.N. Xia, and G.M. Whitesides, Nature **376**, 581 (1995).
33. L.S. Roman, O. Inganäs, T. Granlund, T. Nyberg, M. Svensson, et al., Adv. Mater. **12**, 189 (2000).
34. J.A.E. Wasey, A. Safonov, I.D.W. Samuel, and W.L. Barnes, Phys. Rev. B **6420**, art. no.-205201 (2001).
35. B.J. Matterson, J.M. Lupton, A.F. Safonov, M.G. Salt, W.L. Barnes, and I.D.W. Samuel, Adv. Mater. **13**, 123 (2001).
36. L.S. Roman, W. Mammo, L.A.A. Pettersson, M.R. Andersson, and O. Inganäs, Adv. Mater. **10**, 774 (1998).
37. T. Kugler, W.R. Salaneck, H. Rost, and A.B. Holmes, Chem. Phys. Lett. **310**, 391 (1999).
38. F. Zhang, M. Johansson, M.R. Andersson, J.C. Hummelen, and O. Inganäs, Adv. Mater. **14**, 662 (2002).
39. A. Bietsch and B. Michel, J. Appl. Phys. **88**, 4310 (2000).